Electronic Supplementary Material (ESI) for Journal of Materials Chemistry A.

Supporting Information

Single Nucleation of Cl-doped $FAPbBr_3$ with Inhibited Ion Migration for Ambipolar Radiation Detection

Quanchao Zhang[1], Xin Liu[1]*, Xin Zhang[1], Zijian Wang[1], Baoqiang Zhang[2], Yingying Hao[1], Alain Dubois[1,3], Wanqi Jie[1], Yadong Xu[1]*

[1]State Key Laboratory of Solidification Processing, MIIT Key Laboratory of Radiation Detection Materials and Devices, & School of Materials Science and Engineering, Northwestern Polytechnical University, Xi'an 710072, China

[2]Ametek Co., Ltd., Shaanxi Xixian New Area Qinhan New City Tian Gong 1 road 8-1, Xi'an 712000, China

[3]Laboratory of Physical Chemistry – Matter and Radiation, Sorbonne Université, CNRS-, 75005 Paris France

Corresponding Author

* Tel: +86-29-88460445; Fax: 86-29-88495414

E-mail address: liuxin8@mail.nwpu.edu.cn (X. L.)

E-mail address: xyd220@nwpu.edu.cn (Y. X.).

ORCID

Xin Liu: 0000-0002-0409-1718

Yadong Xu: 0000-0002-1017-9337

Notes

The authors declare no competing financial interest.

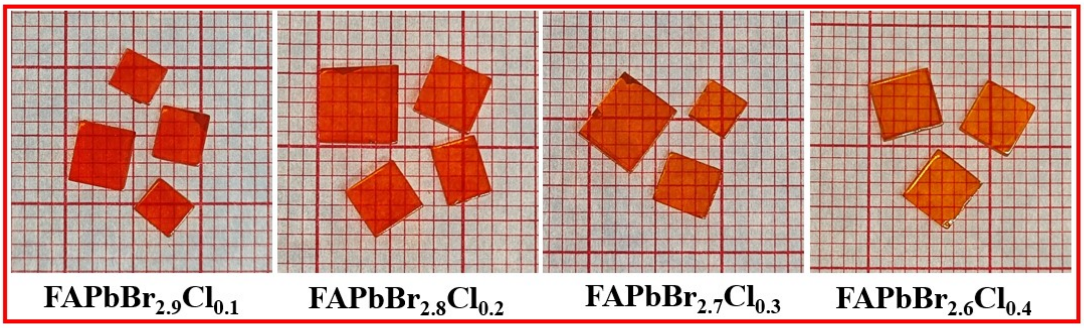

Figure S1. Photos of as-grown $FAPbBr_3$ SCs and $FAPbBr_{3-x}Cl_x$ SCs with Cl/(Cl+Br) ratios varying from 3.3% to 13.3%.

The released expansion stress can be calculated by the formular[1]:

$$\sigma = 8\pi\mu r_{Cl}^{3}\left(\frac{r_{Cl} - r_{Br}}{r_{Br}}\right)^{2}$$

where $\mu = \frac{E}{2(1+\delta)}$ is the shear modulus, E is the Young's modulus, δ is the Poisson's ratio, and r_{Cl} and r_{Br} are the radii of Cl (1.67 Å) and Br (1.84 Å), respectively. Since E(GPa) = -232.25 + 267.06τ where τ is the tolerance factor[2].

Table S3. Tolerance factor of the $FAPbBr_{3-x}Cl_x$ SCs.

Cl	Br	Average radius of halide ion	Pb	FA^+	τ
0	3	0.184			1.0165
0.1	2.9	0.1834			1.0171
0.2	2.8	0.1829	0.12	0.253	1.0176
0.3	2.7	0.1823			1.0182
0.4	2.6	0.1817			1.0188

Notice: the calculation of the tolerance factor can be expressed as:

$$\tau = \frac{r_A + r_X}{\sqrt{2}(r_B + r_X)}$$

where r_A, r_B, r_X is the radius of A site cation (FA^+), B site cation (Pb^{2+}), and halide ion X^-, respectively.

Table S2. EDS component analysis of $FAPbBr_{3-x}Cl_x$ SCs (The average of three points).

	C%	N%	Pb%	Br%	Cl%	Cl: X	Br: Cl
$FAPbBr_3$	30.19	24.65	11.51	33.65	0	-	-
$FAPbBr_{2.9}Cl_{0.1}$	35.09	20.69	11.52	31.56	1.15	3.51	2.89: 0.11
$FAPbBr_{2.8}Cl_{0.2}$	26.20	28.16	11.71	31.91	2.01	5.93	2.82: 0.18
$FAPbBr_{2.7}Cl_{0.3}$	30.34	24.24	11.85	30.03	3.54	10.55	2.68: 0.32
$FAPbBr_{2.6}Cl_{0.4}$	34.40	23.22	10.97	27.26	4.15	13.20	2.60: 0.40

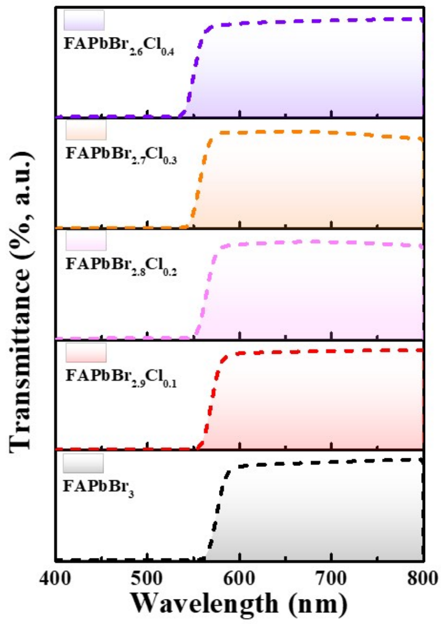

Figure S2. Ultraviolet transmittance spectrum of $FAPbBr_{3-x}Cl_x$ SCs.

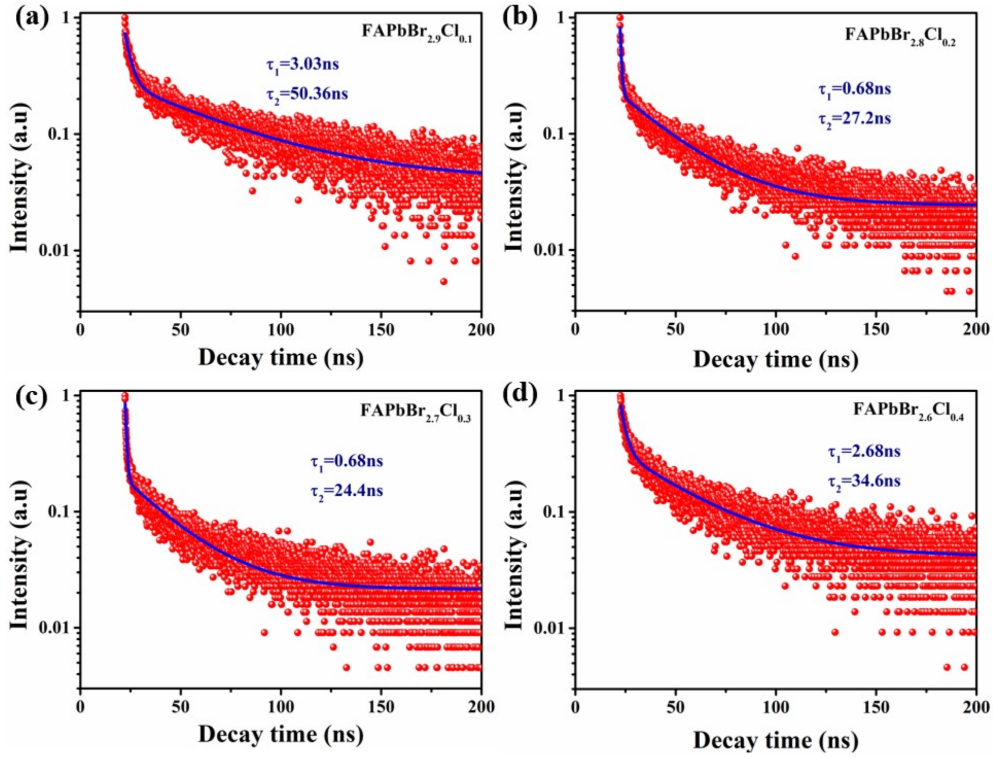

Figure S3. Charge recombination lifetime of $FAPbBr_{3-x}Cl_x$ SCs by TRPL.

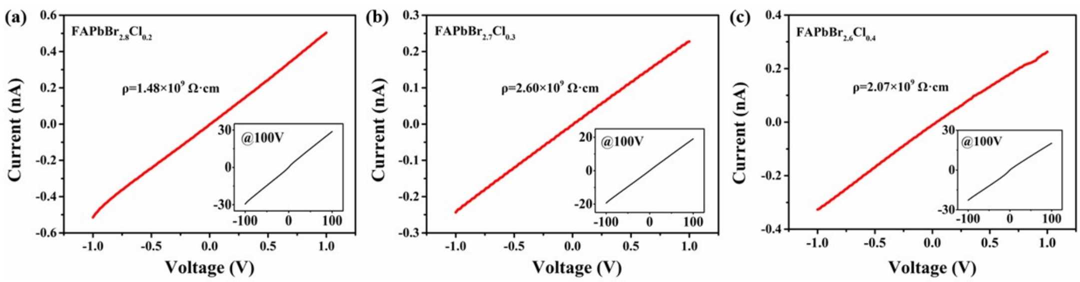

Figure S4. Dark *I-V* curve of (a) Au/$FAPbBr_{2.8}Cl_{0.2}$/Au, (b) Au/$FAPbBr_{2.7}Cl_{0.3}$/Au, (c) Au/$FAPbBr_{2.6}Cl_{0.4}$/Au, devices at room temperature. The inset is the *I-V* curve from -100 V to 100 V.

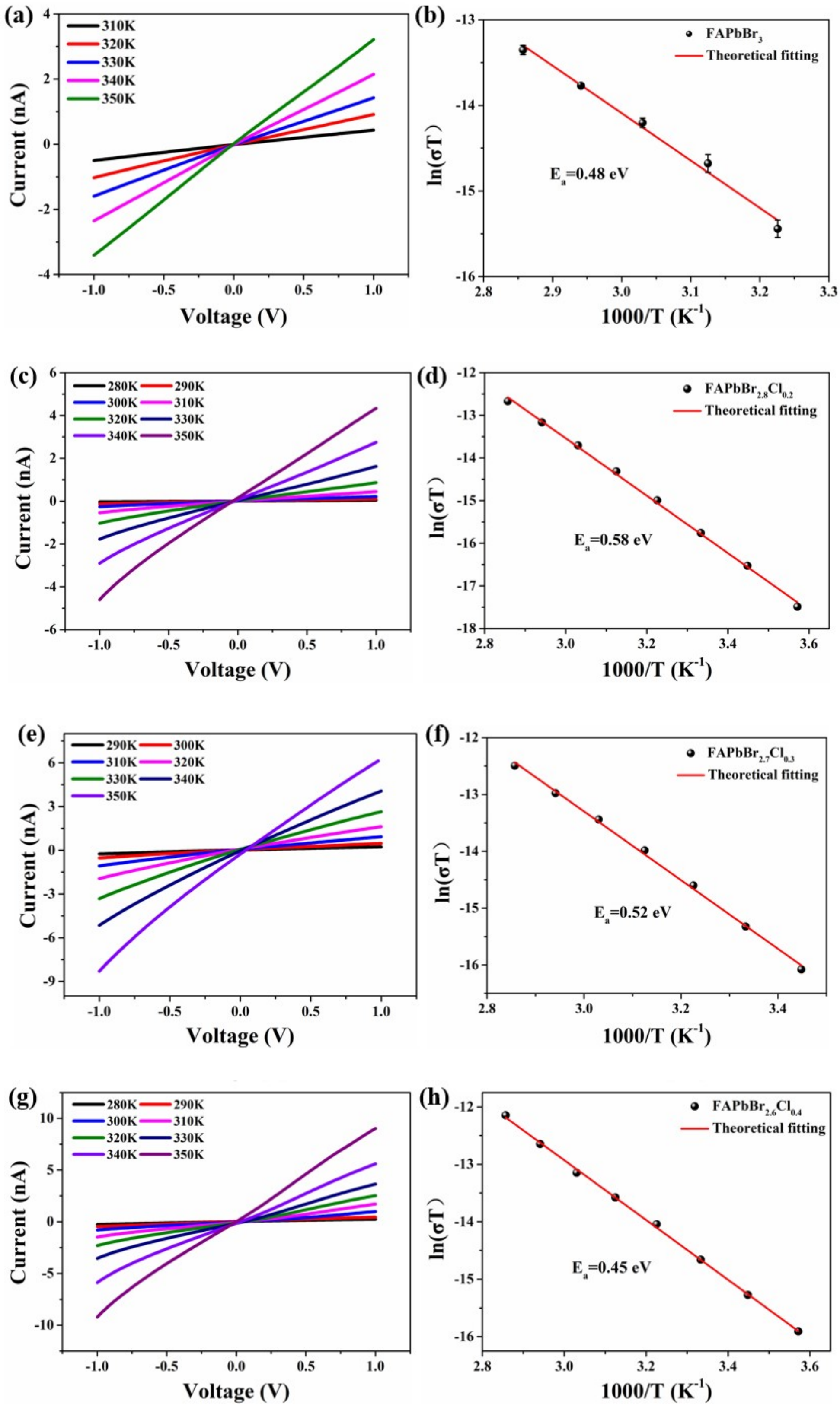

Figure S5. (a)(c)(e)(g) Dark *I-V* curve of Au/ $FAPbBr_{3-x}Cl_x$ /Au devices at different temperatures. (b)(d)(f)(h) Temperature-dependent conductivity measurements of the corresponding $FAPbBr_{3-x}Cl_x$ SCs.

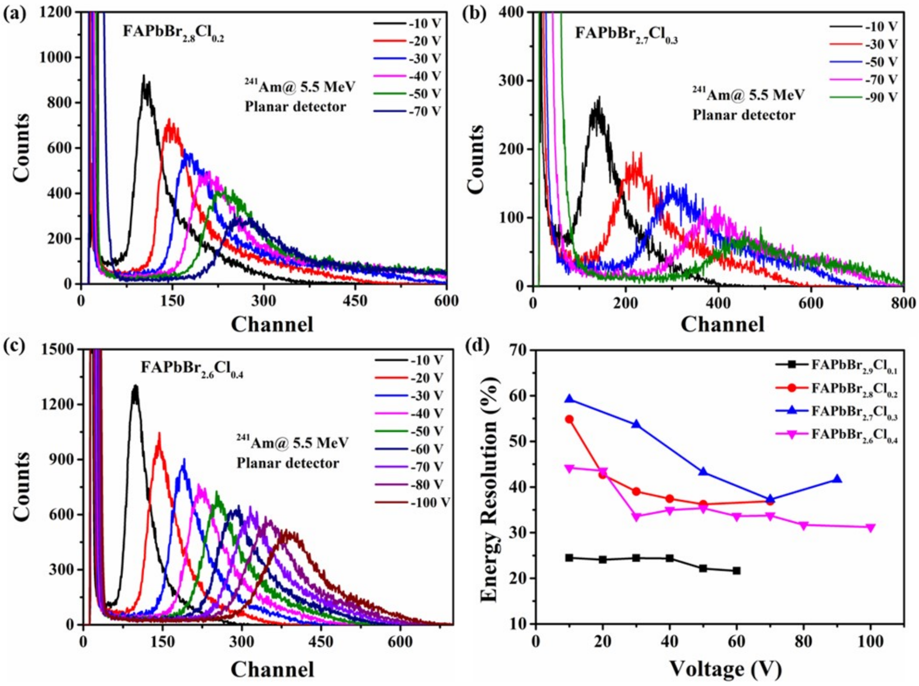

Figure S6. ^{241}Am 5.5 MeV α-particle energy spectra of (a) Au/$FAPbBr_{2.8}Cl_{0.2}$/Au, (b) Au/$FAPbBr_{2.7}Cl_{0.3}$/Au, (c) Au/$FAPbBr_{2.6}Cl_{0.4}$/Au devices under various bias voltages. (d) The comparison of energy resolution of $FAPbBr_{3-x}Cl_x$ SCs under different voltages.

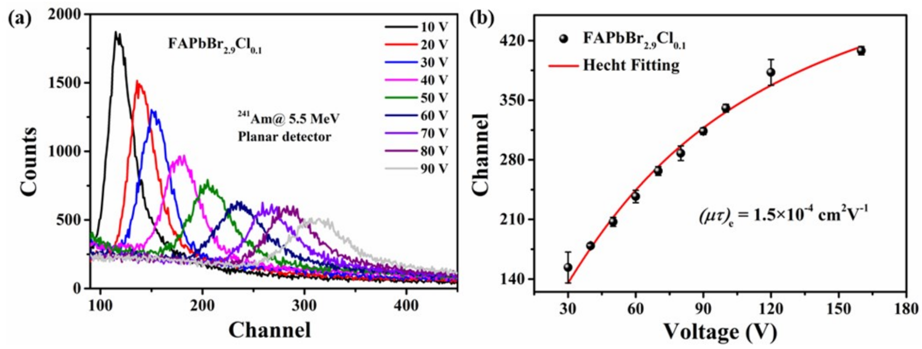

Figure S7. (a) ^{241}Am 5.5 MeV α-particle energy spectra of Au/$FAPbBr_{2.9}Cl_{0.1}$/Au devices under various bias voltages. (b) Electron mobility-lifetime product by Hecht equation fitting.

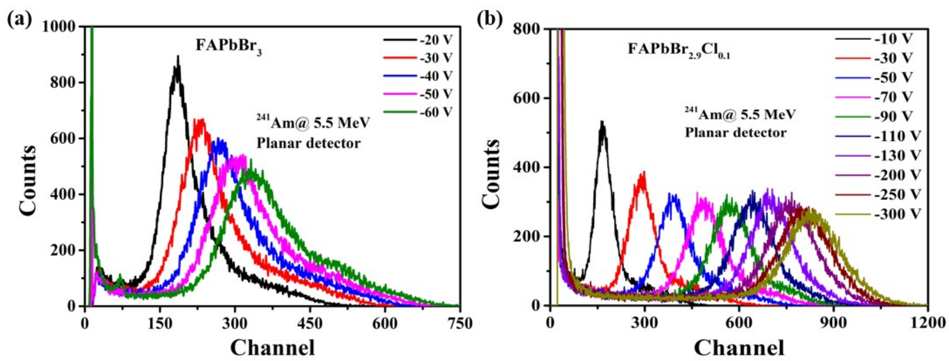

Figure S8. Comparison of voltage resistance: ^{241}Am 5.5 MeV α-particle energy spectra of (a) Au/$FAPbBr_3$/Au, (b) Au/$FAPbBr_{2.9}Cl_{0.1}$/Au devices.

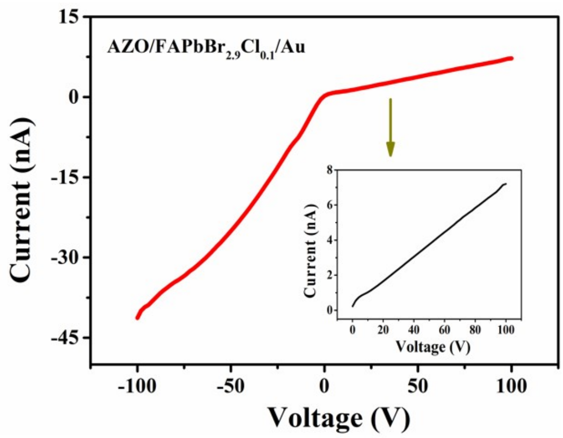

Figure S9. Typical dark *I-V* characteristics of AZO/$FAPbBr_{2.9}Cl_{0.1}$/Au devices.

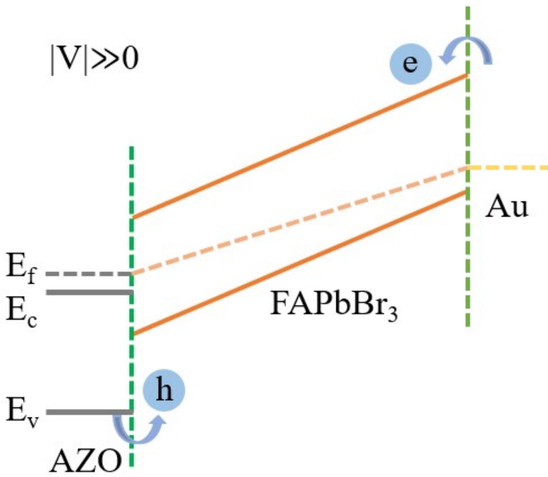

Figure S10 Band diagram of AZO/$FAPbBr_3$/Au

Table S3. Material Properties and Device Performance of Commercialized Radiation Detectors

Materials	Growth method	Band gap (eV)	$\mu\tau$ product ($cm^2\ V^{-1}$)	Maximum Voltage on detector	Energy resolution (%)	Ref.
Ge	Czochralski	0.7	1	1000 V	0.14 (1 MeV/γ-ray)	[3]
CdZnTe	Bridgman	1.57	e: 1.2×10^{-2} h: 9×10^{-5}	200 V	0.8 (662 keV/γ-ray)	[4, 5]
CdZnTe films	Close Spaced Sublimation	1.5	e: 2.562×10^{-4}	50 V	16.45 (5.48 MeV/α particles)	[6]
CdTe	Bridgman	1.44	e: 3×10^{-3} h: 2.6×10^{-4}	600V	12 (662 keV/γ-ray)	[7]
TlBr	traveling molten zone	2.68	e: 3×10^{-5} e: 1.5×10^{-6}	200 V	3.3 (662 keV/γ-ray)	[8]
$FAPbBr_{2.9}Cl_{0.1}$	Inverse temperature crystallization	2.23	e: 2.1×10^{-4} h: 1.5×10^{-4}	300 V	h: 21.3 e: 19.2 (5.48 MeV/α particles)	This work

Reference

[1] H. Ye, Y. Liu, Y. Zhang, et al. Inner Strain Regulation in Perovskite Single Crystals through Fine-Tuned Halide Composition[J]. Crystal Growth & Design, 2021, 21(3): 1741-1750.

[2] S. Sun, Y. Fang, G. Kieslich, et al. Mechanical properties of organic–inorganic halide perovskites, $CH_3NH_3PbX_3$(X = I, Br and Cl), by nanoindentation[J]. Journal of Materials Chemistry A, 2015, 3(36): 18450-18455.

[3] I. Y. Lee, M. A. Deleplanque, K. Vetter. Developments in large gamma-ray detector arrays[J]. Reports on Progress in Physics, 2003, 66(7): 1095-1144.

[4] F. Zhang, Z. He, C. E. Seifert. A Prototype Three-Dimensional Position Sensitive CdZnTe Detector Array[J]. IEEE Transactions on Nuclear Science, 2007, 54(4): 843-848.

[5] F. Liu, R. Wu, J. Wei, et al. Recent Progress in Halide Perovskite Radiation Detectors for Gamma-Ray Spectroscopy[J]. ACS Energy Letters, 2022, 7(3): 1066-1085.

[6] X. Wan, Y. Li, T. Tan, et al. Effects of annealing in Te2 atmosphere on photoelectric properties and carrier transport properties of CdZnTe films[J]. Materials Science in Semiconductor Processing, 2023, 153(107158).

[7] T. T. a. S. Watanabe. Recent Progress in CdTe and CdZnTe Detectors[J]. IEEE TRANSACTIONS ON NUCLEAR SCIENCE, 2001, 48(4).

[8] K. Hitomi, Y. Kikuchi, T. Shoji, et al. Improvement of energy resolutions in TlBr detectors[J]. Nuclear Instruments and Methods in Physics Research Section A: Accelerators, Spectrometers, Detectors and Associated Equipment, 2009, 607(1): 112-115.